INTERNATIONAL JOURNAL OF CLIMATOLOGY
*Int. J. Climatol.* **22**: 451–465 (2002)
Published online in Wiley InterScience (www.interscience.wiley.com). DOI: 10.1002/joc.755

# A SPACE–TIME MODEL FOR SEASONAL HURRICANE PREDICTION

THOMAS H. JAGGER,[a,*] XUFENG NIU[a] and JAMES B. ELSNER[b]
[a] *Department of Statistics, The Florida State University, Tallahassee, FL, USA*
[b] *Department of Geography, The Florida State University, Tallahassee, FL, USA*

*Received 29 May 2001*
*Revised 14 November 2001*
*Accepted 19 November 2001*

## ABSTRACT

A space–time count process model is explained and applied to annual North Atlantic hurricane activity. The model uses the best-track data set of historical hurricane positions and intensities, together with climate variables, to determine local space–time coefficients of a right-truncated Poisson process. The truncated Poisson space–time autoregressive (TPSTAR) model is motivated by first examining a time-series model for the entire domain. Then a Poisson generalized linear model is considered that uses grid boxes within the domain and adds offset factors for latitude and longitude. A natural extension is then made that includes instantaneous local and autoregressive coupling between the grids. A final version of the model is found by backward selection of the predictors based on values of Bayesian and Akiake information criteria. The final model has five nearest neighbours and statistically significant couplings. Hindcasts are performed on the hurricane seasons from 1994 to 1997. Results show that, on average, model forecast probabilities are larger in regions in which hurricanes occurred. Quantitative skill assessment indicates some useful skill above climatology — currently the default leading candidate. The TPSTAR model could be a valuable guidance product when issuing seasonal hurricane forecasts. Copyright © 2002 Royal Meteorological Society.

KEY WORDS: North Atlantic Ocean; space–time Poisson regression; US hurricanes; ENSO; NAO; African rainfall

## 1. INTRODUCTION

Hurricanes are destructive natural phenomena. On average, six or more form each year over the warm tropical and subtropical waters of the North Atlantic. Historically, hurricanes account for a majority of the costliest weather disasters in the USA. They rival earthquakes in destructive potential and loss of life. Despite technological advances in monitoring and prediction, hurricanes retain their potential to cause severe damage and numerous deaths (Arguez and Elsner, 2001). During the 1998 season, hurricane Mitch became a grim reminder that hurricanes can quickly kill thousands of people. In the USA, population and demographic shifts toward the coast are making the problem worse as development flourishes in areas prone to hurricane strikes: the warm subtropical shorelines and islands of the Atlantic Ocean and Gulf of Mexico.

Knowledge of past hurricane occurrences, even if it is incomplete, provides clues about future frequency that goes beyond what present numerical climate models are capable of (Elsner and Bossak, 2001). This understanding is important for land-use planning, emergency management, hazard mitigation, (re)insurance applications and, potentially, the long-term weather derivative market. Climatologists have been issuing seasonal hurricane forecasts for the North Atlantic since 1984 (Gray, 1984; Elsner *et al*., 1996). These forecasts provide total basin estimates of annual counts using linear and generalized linear regression models. Forecasts are issued several months in advance of the season, which runs from June to November, and updated as the season approaches.

* Correspondence to: Thomas H. Jagger, Insightful, 1700 Westlake North, Suite 500, Seattle, WA 98109-3044, USA;
e-mail: tjagger@insightful.com

Some understanding has been achieved in solving the climate puzzle with regard to the question of where hurricanes are likely to go based on conditions a month or two in advance of the season. Lehmiller *et al*. (1997) outline the problem and show the potential for specific forecast models based on regional and large-scale climate factors. Elsner *et al*. (2000) demonstrate a link between the probability of a major hurricane strike on the East Coast and the strength of the North Atlantic oscillation (NAO). Physically, it is reasoned that the strength of the NAO is an indication of the position and strength of the subtropical high, which steers hurricanes toward or away from the coast. Taking advantage of a unique wind speed data set derived from hurricane landfalls in the USA, Jagger *et al*. (2001) developed a model for hurricane probabilities conditioned on climate anomalies, including El Niño and the NAO.

However, current seasonal forecast models for the entire North Atlantic basin do not incorporate spatial and temporal information. Thus they fail to provide specific seasonal activity forecasts for different geographic regions of the hurricane basin, which includes the Gulf of Mexico and Caribbean Sea. Statistical models need to be created that combine spatial and temporal correlation in the data to generate regional forecasts. This paper introduces a class of space–time statistical models for count data that can be used for seasonal hurricane prediction. Ultimately the goal is a model that can predict the likely tracks of hurricanes for an entire season.

The paper is organized as follows. Sections 2 and 3 describe the data and model grid respectively. Model formulae and justification are presented in Section 4, along with a description of the model predictors. Section 5 describes increasingly sophisticated models as a way to understand the full model. Final model selection procedures are given in Section 6. Model fit issues and hindcasts are provided in Section 7, and the summary and list of conclusions are given in Section 8.

## 2. DATA

Hurricanes are tropical cyclones with maximum sustained winds reaching 65 kt or greater. Hurricane positions and intensities are obtained from the best-track records (Neumann *et al*., 1999), which are a compilation of the six-hourly information of all tropical cyclones back to 1886. Hurricane records are most reliable beginning with the use of aircraft reconnaissance in 1944. Before this time some hurricanes may have gone undetected, especially in regions of the open North Atlantic Ocean away from the principal shipping lanes and populated islands. The annual average number of North Atlantic hurricanes over the period 1900–43 is 3.9. This compares with an annual average of 5.7 over the period 1944–93. The degree to which this difference in mean hurricane rates is due to improved observations against a backdrop of climate variability is open to considerable debate. Neumann *et al*. (1999) note that the confluence of the typical cyclone tracks with shipping lanes and populated islands makes it unlikely that major storms would have missed detection even back into the 19th century. They add that, without additional observations, the centre location and strength estimates are less accurate. At present, a more quantitative analysis that compares hurricane records and meta data from before and after 1944 to assess the level of bias is lacking.

Since it is important to use long records in statistical modelling, here we compare the spatial intensity of hurricane (significant tropical cyclone) positions between the two periods. Figure 1 contains plots of spatial hurricane intensity grouped by time periods and by initial and final positions. The plots are constructed by counting the hurricane positions in 5° latitude by longitude boxes. Box counts are smoothed using a local regression with a span of 10% in both cardinal directions. For the initial positions, the spatial intensity maps are quite similar, with most hurricanes forming between 50 and 90°W longitude and between 15 and 30°N latitude. During the later period, more hurricanes are detected at higher latitudes between 40 and 65°W longitude. The spatial intensity maps of final hurricane positions also show similarities between the two time periods. However, here the greatest concentration shifts from the Gulf of Mexico during the earlier period to off the northeast coast of the USA during the later period. This shift is consistent with better detection of hurricanes over the open ocean since the time of aircraft reconnaissance.

However, the shift is also consistent with a climate change featuring more recurving hurricanes since the mid 20th century. In fact, we can use US hurricane landfalls from North Carolina to Maine as a proxy for recurving hurricanes (landfall reports are reliable back to at least 1900). We find an average of 0.23 hits

 

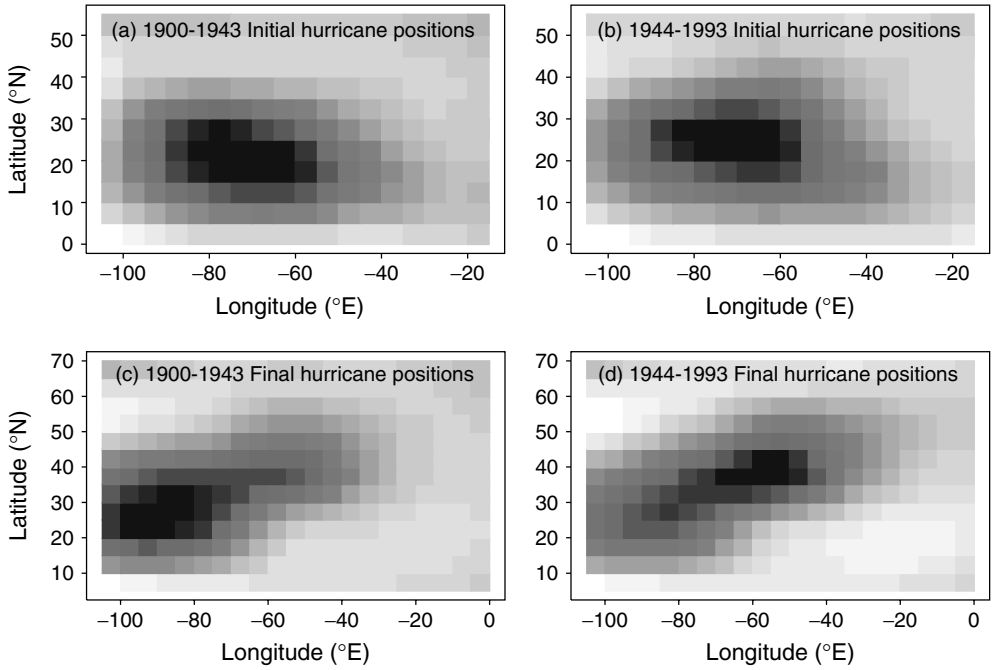


Figure 1. Spatial intensity maps of hurricane positions. Initial hurricane positions over the period (a) 1900–43 and (b) 1944–93. Final hurricane positions over the period (c) 1900–43 and (d) 1944–93. The maps are made by counting the number of positions within each 5° latitude by 5° longitude box and using a local regression smoother with a span of 10%. Darker boxes indicate more hurricanes

(each hurricane is counted only once) per year during the earlier period and an average 0.36 hits during the later period. This amounts to an 88% increase in the annual odds of a hurricane along the northeast coastline resulting from an increase in the occurrence of recurving hurricanes. Thus it is likely that the differences noted in the spatial intensity maps of final hurricane positions are, to an extent, related to actual climate variability. Although this limited comparison does not prove the reliability of the earlier years, it does provide confidence that the models used and developed in this paper will not be overly influenced by a potential data bias.

## 3. MODEL GRID

To develop the model we divide the North Atlantic basin into a $6^\circ \times 6^\circ$ latitude and longitude grid. Data are annual hurricane counts in the grid boxes. A tropical cyclone that records a position at hurricane strength within the box is counted once. A hurricane that loops around and re-enters the box is counted as a single hurricane. Grid choice is a compromise between sample size and resolution. As noted later, model coefficients are estimated using a Monte Carlo procedure, and the procedure fails to converge for smaller grid boxes because between grid box correlations are too large.

We remove grids having mostly land or historically low hurricane activity, leaving grid $S$ with 40 cells as shown in Figure 2. Total hurricane occurrences over the 94 year period are shown for each region. Historically, hurricane activity is most pronounced over the Bahamas, extending north and eastward toward Bermuda (see Elsner and Kara 1999). Count values in the grid boxes outside region $S$ are used as boundary conditions for the model. This improves the estimates of model constants over the case where the boundary values must be assumed or estimated. For generating hindcasts we set the boundary values equal to zero to approximate annual climatology.

Count values in the grid boxes obtained from the best-track data and used in model development are displayed as a series of space–time images in Figure 3. Each image represents an $11 \times 8$ grid ($6^\circ \times 6^\circ$ latitude–longitude), covering the western half of the North Atlantic for a single season. Grey levels in the

 

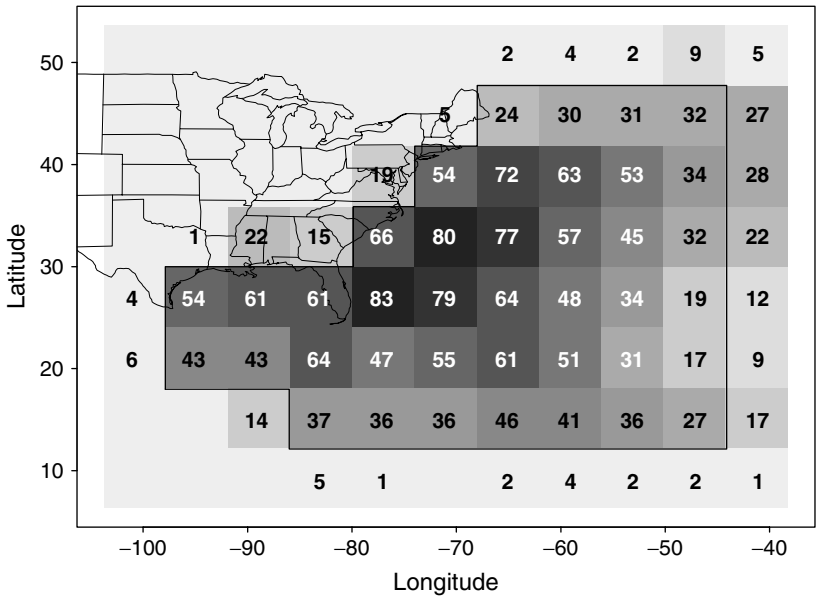


Figure 2. Grid boxes indicate the total number of hurricanes over the period 1900–93. The black line (region *S*) outlines the 40 grid boxes used in the model. Hurricane activity in the surrounding boxes is used as boundary conditions

images indicate the number of hurricanes whose centres pass into the region during the year. Activity in the grids ranges from zero (light grey) to four (black). Low-latitude hurricane activity dominated the region during 1916 and 1933, whereas high-latitude activity was more pronounced during 1963 and 1969. Note that there are no hurricanes in the best-track data for the years 1907 and 1914. Seasonal hurricane counts are used as the model response, as detailed next.

## 4. A RIGHT-TRUNCATED POISSON SPACE–TIME MODEL

Hurricane frequencies over time and space form a space–time counts process. The dependence structure of this type of data can be modelled by a conditional probability approach (Whittle, 1963; Bartlett, 1968; Besag, 1974; Gilks *et al*., 1996). Besag (1974) introduced conditionally specified auto-Poisson models for spatial counts data, which link observation of a Poisson process at a given location with those at its spatial neighbourhoods. However, the auto-Poisson model proposed by Besag (1974) has restrictions on the parameter space, making it applicable only to spatial data in which the interaction coefficients are non-positive. Here we consider a class of space–time regression models for hurricane activity based on the right-truncated Poisson distribution

$$\Pr(H = x) = \frac{\lambda^x}{x! \sum_{w=0}^{M} (\lambda^w / w!)} \quad x = 0, 1, \ldots, M \tag{1}$$

where $M$ is an upper bound for the annual number $H$ of hurricanes occurring in a given grid box during any given year. The truncated Poisson space–time autoregressive (TPSTAR) model we propose allows the coupling parameters for neighbouring sites to take on positive values.

We restrict the specification to a spatially invariant, nearest neighbour, first-order autoregressive model, with predictors. The space–time neighbourhood consists of five sites: north, south, east, west, and the previous season's activity at the given site, as shown in Figure 4. Note that using the TPSTAR model

 

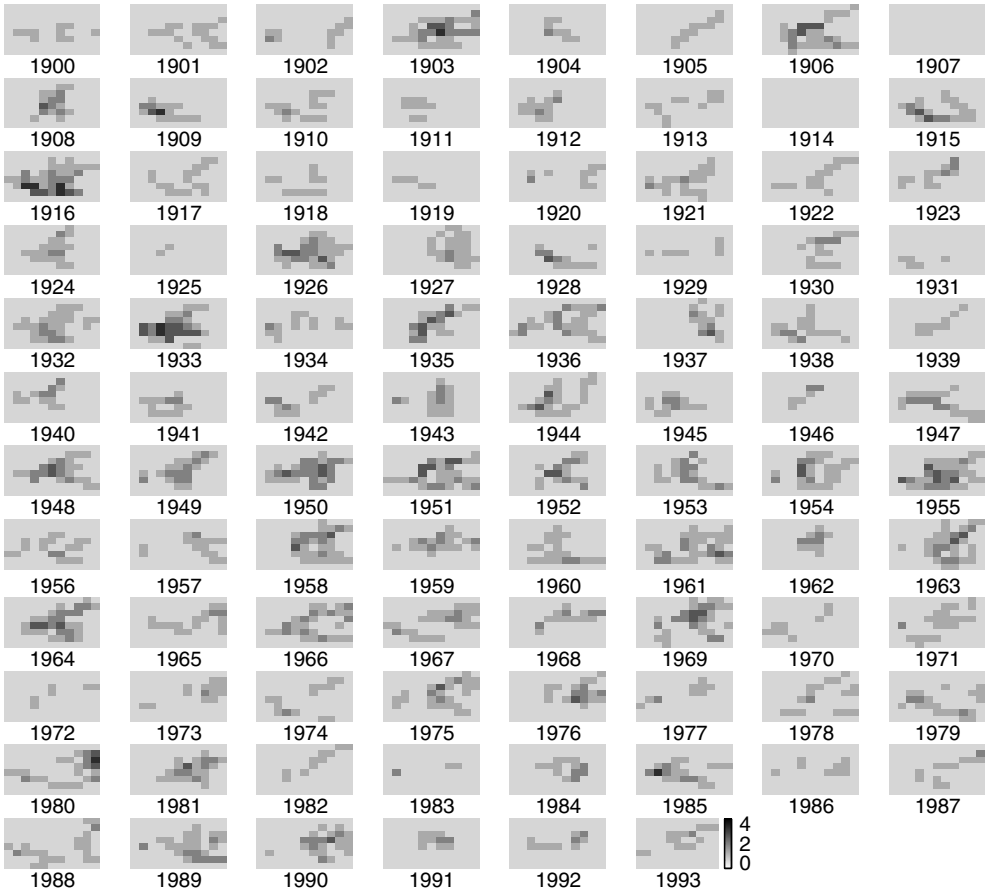


Figure 3. Hurricane activity over the North Atlantic by region and year (1900–93). Grey intensities indicate the level of activity in $6^\circ \times 6^\circ$ grid boxes over the western half of the basin

on this neighbourhood requires three coupling parameters $\gamma_{0h}$, $\gamma_{0v}$, $\gamma_{1c}$ for the east–west, the north–south and the temporal lag-one coupling respectively.

Each grid box $(t, ij)$ represents a $6^\circ \times 6^\circ$ region for 1 year. Let the response values $H_{t,ij}$ be the number of distinct hurricanes passing into any portion of the grid $(i, j) \in S$ during year $t$. The location centres of each grid box shown in Figure 2 have longitude given by $-101^\circ + 6^\circ \times i$ for $i = 0, 1, \ldots, 10$ and latitude given by $9^\circ + 6^\circ \times j$ for $j = 0, 1, \ldots, 7$. Region $S$ has $i = 1, 2, \ldots, 9$ and $j = 1, 2, \ldots, 6$.

We can describe the distribution model conditionally as:

$$\forall ij \in S : H_{t,ij} | h_{\partial\{(t,ij)\}} \sim \text{tpois}(\lambda_{t,ij}, M) \tag{2}$$

where $h_{\partial(t,ij)}$ is the vector of five response values, $h_{t,i-1,j}$, $h_{t,i+1,j}$, $h_{t,i,j-1}$, $h_{t,i,j+1}$ and $h_{t-1,i,j}$, in the neighbourhood of the location $(t, i, j)$, and tpois is the right-truncated Poisson distribution with rate $\lambda_{t,ij}$ truncated at $M$. For the neighbourhood system shown in Figure 4, the TPSTAR model has the form:

$$\log(\lambda_{t,ij}) = C_{ij}(t) + \gamma_{0h}(H_{t,i+1,j} + H_{t,i-1,j}) + \gamma_{0v}(H_{t,i,j+1} + H_{t,i,j-1}) + \gamma_{1c}(H_{t-1,i,j}) \tag{3}$$

where

$$C_{ij}(t) = \alpha_{ij} + \sum_{k=1}^{p} b_k z_k(t)$$

with $b_k$ the coefficient for the $k$th yearly covariate and $\alpha_{ij}$ the grid $ij$ offset.

 

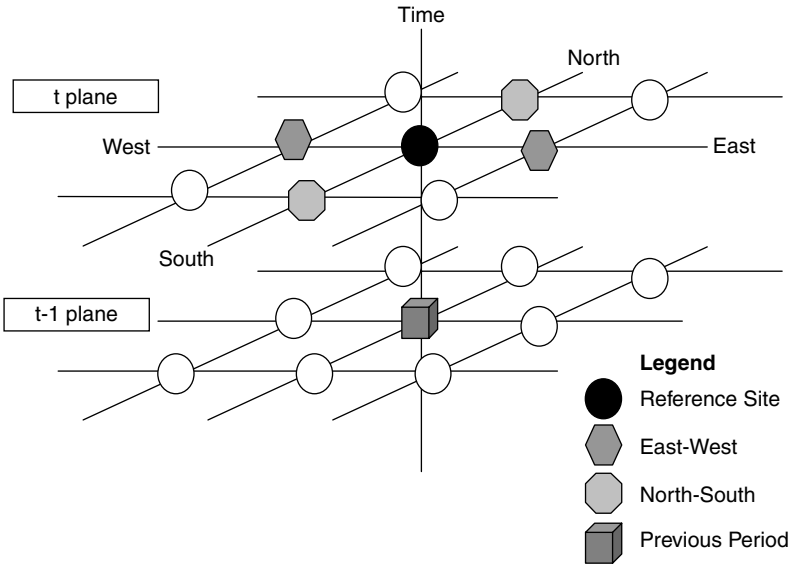


Figure 4. The space–time neighbourhood of the reference grid box (site) used to model annual hurricane activity. The shaded objects indicate grid boxes used in the model. The previous period represents last year's hurricane activity in the grid box of interest

We chose $M = 10$ for the grid boxes, since it is larger than the maximum number of hurricanes observed in any grid box per year. The value of $M$ is small enough to observe positive coupling, yet large enough to compare the results of this model with models based on the Poisson distribution.

The model makes use of three predictor types:

(1) neighbourhood response values or coupling grid box frequencies,
(2) local offsets, represented by $\alpha_{ij}$, and
(3) yearly global covariates denoted by $z_k(t)$.

Predictors of type (1) concern neighbourhood hurricane frequencies with parameters $\gamma_{0h}$, $\gamma_{0v}$, and $\gamma_{1c}$, indicating the east–west, north–south, and autoregressive lag-one couplings respectively.

Predictors of type (2) represent the regional effects from predictors that are not measured at each location, such as sea surface temperature, location with respect to land mass, and the variation in surface area from region to region. The parameters are given by $\alpha_{ij}$. Without additional information the site offset gives an indication of average yearly activity in the associated grid box. As $\alpha_{ij}$ represents one parameter for every grid box, this can be a considerable number of parameters. Thus, we constrain $\alpha_{ij}$ to be the sum of two factors longitude $\text{long}_i$ and latitude $\text{lat}_j$ where $\alpha_{ij} = \text{con} + \text{long}_i + \text{lat}_j$ with the sum constraints $\sum_{i=1}^{\text{lg}N} \text{long}_i = 0$ and $\sum_{j=1}^{\text{lt}N} \text{long}_j = 0$ where con is a constant, i.e. the intercept, and lg$N$ and lt$N$ are the number of longitude (nine), and latitude (six) regions. This reduces the number of parameters associated with offsets from 40 to 14 in the present case. Since $\text{long}_9$ and $\text{lat}_6$ are determined by the sum constraints, they are not reported.

Predictors of type (3) represent the climate covariates as identified by previous research studies (Jagger *et al*., 2001). Here we consider the influence of the covariate to be the same across grid boxes, and allow the value of the covariate to vary in intensity from year to year. The number of covariates is restricted by data availability. The climate covariates used in the TPSTAR model include the following.

*Warm & Cold*. 'Warm' and 'Cold' refer to the state of the El Niño–southern oscillation (ENSO), which is the aperiodic warming and cooling of the ocean mixed-layer waters over the equatorial central and eastern tropical Pacific and their associated atmospheric interaction. This factor takes three values in the model: 'Warm', +1 representing an El Niño event; 'Cold', −1, representing a La Niña event or 0 for neither event. Definitions and values are given in Elsner *et al*. (1998). Shapiro (1987) demonstrates that wind speeds at levels above the tropical North Atlantic are correlated to the phase of the ENSO. Since stronger winds in the

 

upper atmosphere are related to increased wind shear over areas of tropical storm development, the presence or absence of El Niño is an indicator of the level of hurricane activity over the North Atlantic.

*Dakar*. 'Dakar' refers to annual rainfall over Dakar, Senegal. Landsea and Gray (1992) show a correlation between North Atlantic hurricane activity and rainfall during the West African rainy season. It is speculated that above-normal rainfall in this region is a signal that sea surface temperatures over the tropical North Atlantic are above normal and that, therefore, the adjacent ocean waters will likely spawn more tropical storms and hurricanes.

*Azores*. 'Azores' refers to annual sea level pressure (SLP) in the Azores given in millibars. SLP over the Azores is an indication of the strength and position of the subtropical high-pressure zone.

*Iceland*. 'Iceland' refers to annual SLP in Iceland given in millibars. Elsner and Kara (1999) note that lower pressures are favourable for hurricane formation, either by reduced wind shear due to relaxed trades or baroclinic enhancement from weak low-pressure eddies in the sub-tropics generated by major mid-latitude troughs. The difference in SLP between Iceland and the Azores (Iceland − Azores) represents the NAO. Elsner *et al*. (2000) show that major hurricanes along the northeast coast of the USA are more likely under a strong, positive NAO.

## 5. COMPARING MODELS

To examine better the hurricane activity as a count process over the basin, we present results from three different models: a time-series only model, a space–time model without instantaneous coupling parameters, and a full model with coupling parameters. The full model given in Equation (3) represents a version of TPSTAR. The first two models are fit to a Poisson generalized linear model (GLM) with dispersion. To fit the full model we try both a maximum Poisson likelihood estimator (MPLE) and a Monte Carlo maximum likelihood estimator (MCMLE).

The MPLE extends the GLM model by adding neighbourhood observations as covariates to the models. If the covariate matrix is of full rank, the MPLE using the canonical link function always produces a parameter estimate. If the model is shift invariant with finite range, the parameter estimates of the MPLE are asymptotically consistent with increasing domains (Winkler, 1995). However, even in the shift invariant case, the MPLE is not necessarily efficient, and does not provide standard error estimates. We use the MCMLE method for consistent and efficient parameter estimates with consistent parameter covariance estimates as described in Geyer (1994) and used by Wu (1994). The MCMLE method was extended by Jagger (2000) to handle the autoregressive coupling in the TPSTAR model.

The MCMLE method has several problems. For one, it is computationally intensive as it uses a Markov chain Monte Carlo method for estimating the log likelihood function. For another, the method fails to converge, unless the initial parameter estimates are close to the actual parameter values. Though the MPLE is biased in our case, the convergence problem is somewhat alleviated by using the MPLE for initial parameter estimates.

For the time-series model, we analyse annual hurricane counts over the entire region $S$. The time series for 95 years $H_t$, $t \in 1889 \cdots 1993$, is shown in Figure 5. $H_t$ represents the number of separate hurricanes passing through any portion of the region in year $t$. Although not all predictors are significant in the time-series formulation, we compare the parameter values and their errors with values obtained after dividing the region into $6^\circ \times 6^\circ$ grid boxes.

Table I shows the parameter estimates from the time-series model. The formulation is a Poisson GLM with dispersion. A Poisson GLM is used on US hurricane activity by Elsner and Bossak (2002) and Elsner *et al*. (2001). We note that the model is somewhat under-dispersed. The dispersion is estimated from the Pearson statistic $\sum_{t=1}^{n} [(H_t - f_t)/\mathrm{SE}(f_t)]^2$ where $f_t$ is the fitted value for $H_t$ and $\mathrm{SE}(f_t)$ is the standard error of $f_t$. Dakar rainfall, Azores pressure, and the warm phase of the El Niño are significant at $\alpha = 0.05$, but the autoregressive coefficient is not.

Table II shows the parameter estimates for a Poisson GLM with dispersion after modifying the time-series model by dividing the basin into grids, and adding the offset factors for latitude and longitude. In other words,

 

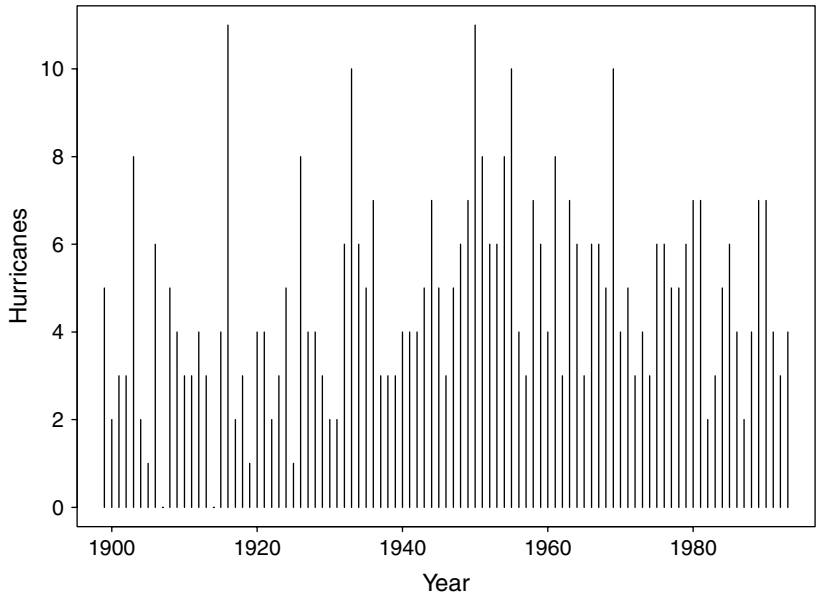


Figure 5. Annual hurricane counts over the region $S$ during the period 1889–1993, inclusive. Although we only model the seasons from 1900–93, the model requires previous year's activity. Region $S$ is shown as a black outline in Figure 2

Table I. Parameter estimates and statistics for the time-series model. The dispersion parameter estimate is 0.924; residual deviance is 87.0 with 87 degrees of freedom. There are 94 observations, with $\sum_{t=0}^{93} H_{t+1900} = 424$

| | Value | Standard error | $t$ value | Units |
|---|---|---|---|---|
| Intercept | 198.475 | 68.996 | 2.88 | |
| $\gamma_{1c}$ | 0.037 | 0.0194 | 1.88 | |
| Cold | 0.193 | 0.108 | 1.78 | |
| Warm | −0.302 | 0.126 | −2.38 | |
| Dakar | 0.594 | 0.250 | 2.40 | years per metre |
| Azores | −0.149 | 0.049 | −3.05 | per millibar |
| Iceland | −0.046 | 0.027 | −1.71 | per millibar |

the fitted model has the expression in Equation (3) with $\gamma_{0h} = \gamma_{0v} = \gamma_{1c} = 0$ and $\alpha_{ij} = \text{con} + \text{long}_i + \text{lat}_j$. The associated $t$ values on the model coefficients indicate that every factor is significant at $\alpha = 0.05$. The fact that the lag-one autoregressive coefficient is significant is unexpected, since it was insignificant in the time-series model. Variances for the global predictors are significantly smaller than the variance of the time series model. Thus, the $t$ values on the global predictors in the second model are about three times those in the first model.

Conclusions about the parameters and their standard errors are not entirely valid, as the GLM assumes no instantaneous coupling; that is, the conditional distribution given the past is independent for each site. This assumption does not hold because our data consist of hurricanes that pass between adjacent grid boxes, creating correlations in annual counts between adjacent boxes. This suggests adding spatial structure to the model in the form of coupling parameters. Note that the GLM formulation does not require temporal independence, since the assumed MLE in the GLM estimator is the same as the actual MLE for an autoregressive time series. Thus, in the absence of instantaneous coupling, we can use the Poisson GLM and treat past values of the response as covariates in the model.

 

Table II. Parameter estimates and statistics for the Poisson GLM. The dispersion parameter estimate is 0.966; residual deviance is 3536.38 on 3740 degrees of freedom. There were 3760 observations with $\sum_{t,ij} H_{t,ij} = 1924$

| | Value | Standard error | $t$ value | Units |
|---|---|---|---|---|
| $\gamma_{1c}$ | 0.094 | 0.028 | 3.34 | per hurricane |
| Intercept | 244.823 | 34.009 | 7.19 | |
| $\text{lat}_1$ | 0.101 | 0.040 | 2.53 | |
| $\text{lat}_2$ | 0.097 | 0.020 | 4.92 | |
| $\text{lat}_3$ | 0.070 | 0.016 | 4.44 | |
| $\text{lat}_4$ | 0.035 | 0.013 | 2.62 | |
| $\text{lat}_5$ | −0.067 | 0.016 | −4.16 | |
| $\text{long}_1$ | 0.034 | 0.069 | 0.50 | |
| $\text{long}_2$ | 0.052 | 0.035 | 1.49 | |
| $\text{long}_3$ | 0.023 | 0.022 | 1.07 | |
| $\text{long}_4$ | 0.016 | 0.015 | 1.10 | |
| $\text{long}_5$ | 0.012 | 0.011 | 1.04 | |
| $\text{long}_6$ | −0.014 | 0.010 | −1.49 | |
| $\text{long}_7$ | −0.038 | 0.009 | −4.23 | |
| $\text{long}_8$ | −0.068 | 0.009 | −7.36 | |
| Warm | −0.391 | 0.064 | −6.12 | |
| Cold | 0.293 | 0.052 | 5.66 | |
| Dakar | 1.260 | 0.120 | 10.47 | year per metre |
| Azores | −0.193 | 0.029 | −8.12 | per millibar |
| Iceland | −0.049 | 0.013 | −3.66 | per millibar |

Model estimates for the final model are derived using the results of a pseudo likelihood estimator as inputs to the MCMLE. The MCMLE is then run iteratively with 1000 samples at each stage. Table III shows the MCML estimates of the parameters in Equation (3) after four iterations of the estimator. Parameter estimates converge with changes between the third and fourth iteration of less than 0.6 times the estimated standard error. The root-mean-square change is $0.20\sigma$.

Results from the full TPSTAR model indicate all couplings are positive and significant. Note again that the lag-one coupling, which was not significant in the time-series model, is significant in the space–time model. This is a new finding that provides evidence for hurricane path persistence over successive years. Locations that were threatened by a hurricane one year are more likely to be threatened again in the next year. As with the second model, the climate predictors are significant.

Estimates from the MCMLE appear to be reasonable. The model takes into consideration both spatial and temporal couplings. For example, the parameter estimates are the same sign but smaller in the final model with instantaneous couplings compared with the Poisson GLM without instantaneous couplings, or the time-series model. This makes sense, since a positive coupling causes the expected value of any statistic to be more sensitive to changes in the predictor value than would be expected in the absence of the coupling. The parameters and the estimated standard errors from the modified MCMLE are smaller than those obtained with the first two models. This reduction in standard error might be real owing to the addition of instantaneous coupling and offsets, but it is more likely an artifact of the apparent increase in total hurricane counts from 435 in the time series model to 1676 in the TPSTAR model.

Table IV shows the estimated correlations between the coupling parameters and model intercept. The correlations between the temporal and spatial coupling parameters are small, whereas the correlation between the east–west and north–south coupling parameters are considerably larger. Surprisingly the intercept is not strongly correlated to the coupling parameters.

 

Table III. Parameter estimates and statistics for the TPSTAR model

| | MPLE | MCMLE | | | Units |
|---|---|---|---|---|---|
| | Value | Value | Standard error | $t$ value | |
| $\gamma_{0h}$ | 0.389 | 0.358 | 0.014 | 24.90 | per hurricane |
| $\gamma_{0v}$ | 0.250 | 0.287 | 0.017 | 16.75 | per hurricane |
| $\gamma_{1c}$ | −0.002 | 0.079 | 0.020 | 4.03 | per hurricane |
| Intercept | 57.412 | 148.537 | 18.473 | 8.04 | |
| $\text{lat}_1$ | −0.072 | −0.010 | 0.038 | −0.27 | |
| $\text{lat}_2$ | 0.012 | 0.023 | 0.017 | 1.35 | |
| $\text{lat}_3$ | 0.039 | 0.022 | 0.013 | 1.74 | |
| $\text{lat}_4$ | 0.044 | 0.007 | 0.011 | 0.60 | |
| $\text{lat}_5$ | −0.012 | −0.047 | 0.013 | −3.62 | |
| $\text{long}_1$ | −0.197 | −0.116 | 0.076 | −1.53 | |
| $\text{long}_2$ | −0.056 | −0.003 | 0.035 | −0.09 | |
| $\text{long}_3$ | −0.047 | −0.009 | 0.020 | −0.45 | |
| $\text{long}_4$ | −0.042 | −0.009 | 0.013 | −0.68 | |
| $\text{long}_5$ | −0.024 | −0.013 | 0.010 | −1.32 | |
| $\text{long}_6$ | −0.024 | −0.032 | 0.009 | −3.73 | |
| $\text{long}_7$ | −0.018 | −0.039 | 0.008 | −4.77 | |
| $\text{long}_8$ | −0.037 | −0.055 | 0.008 | −6.79 | |
| Warm | −0.124 | −0.230 | 0.038 | −6.02 | |
| Cold | 0.072 | 0.192 | 0.027 | 7.15 | |
| Dakar | 0.368 | 0.768 | 0.068 | 11.31 | year per metre |
| Azores | −0.042 | −0.120 | 0.013 | −9.14 | per millibar |
| Iceland | −0.015 | −0.028 | 0.007 | −3.96 | per millibar |

Table IV. Parameter correlations for TPSTAR model

| | $\gamma_{0,h}$ | $\gamma_{0,v}$ | $\gamma_{1,c}$ | Intercept |
|---|---|---|---|---|
| $\gamma_{0h}$ | 1.000 | −0.763 | −0.075 | −0.022 |
| $\gamma_{0v}$ | −0.763 | 1.000 | 0.003 | −0.084 |
| $\gamma_{1c}$ | −0.075 | 0.003 | 1.000 | 0.103 |
| Intercept | −0.022 | −0.084 | 0.103 | 1.000 |

## 6. MODEL SELECTION

Backward elimination is applied to the TPSTAR model to arrive at a final model of the spatial–temporal variations in seasonal hurricane activity. The procedure makes use of the estimated changes in the Schwartz's Bayesian information criteria (SBC) and the Akaike information criteria (AIC). In fact, we need to use changes in criterion levels because the TPSTAR model generates rough estimates of the deviance or predicted values. Thus, common statistics for model selection cannot be calculated accurately. The deviance requires knowledge of the normalizing constant for the distribution, which cannot be estimated accurately in the presence of strong coupling.

We test significance with the Wald test, and use this to compare the difference in SBC or AIC between two models. Both AIC and SBC are used for model selection. Although no asymptotes for either of these statistics exist for our model, for a stationary Gaussian time series, minimizing the AIC gives a model with the smallest predictive error, whereas minimizing the SBC gives a consistent model (Brockwell and Davis, 1991, pages 301–6).

Assume we have two nested models with the second model generated from the first by adding an additional factor with $q$ levels, for a total of $p$ parameters. Let $\boldsymbol{\theta} = [\boldsymbol{\theta}_1, \ldots, \boldsymbol{\theta}_q]$ be the parameter vector

 

with $\boldsymbol{\theta} \in \mathrm{R}^p$ and $\boldsymbol{\theta}_q \in \mathrm{R}^q$ for the added factor. Let $\boldsymbol{\Sigma}_q$ be the covariance matrix for the added factor, then the Wald test is $H_0 : \boldsymbol{\theta}_q = 0$ and the statistic $W = \boldsymbol{\theta}_q' \boldsymbol{\Sigma}_q^{-1} \boldsymbol{\theta}_q$, and asymptotically in $n$, $W$ has a $\chi^2$ distribution with $q$ degrees of freedom. Since $\mathrm{AIC} = -2 \log \ell(\boldsymbol{\theta}) + 2p$ and the asymptotic distributions for $W$ and $2 \log \ell(\boldsymbol{\theta}) - 2 \log \ell(\boldsymbol{\theta}_1)$ are equal, we can approximate the change in AIC for adding the factor with $q$ levels as $\Delta\mathrm{AIC}_\mathrm{F} \approx -W + 2q$. Since $\mathrm{SBC} = -2 \log \ell(\boldsymbol{\theta}) + p \log(n)$, the change in SBC for adding a factor with $q$ levels is $\Delta\mathrm{SBC}_F \approx -W + q \log(n)$. Now, if we remove a factor with $q$ levels then the changes in the information are $\Delta\mathrm{AIC}_B \approx W - 2q$ and $\Delta\mathrm{SBC}_B \approx W - q \log(n)$.

Let us consider four versions of the TPSTAR model with instantaneous coupling. The first version is without offsets, so it has three coupling parameters, the intercept, and five climate covariates, giving a total of $p_1 = 9$ parameters. Version two adds the longitude factor, increasing the number of parameters to $p_2 = p_1 + 8 = 17$. Version three adds the latitude factor to model one, increasing the number of parameters to $p_3 = p_1 + 8 = 14$. Version four adds both factors to the original model for a total of $p_4 = p_1 + 8 + 5 = 22$ parameters. First, we test the estimated change in SBC excluding the latitude factor or longitude factor. If the change is negative for either factor we remove this factor from the model. Then we rerun the model and test the change in SBC and AIC by removing the other offset factor. Table V shows these results, which indicate removing the latitude factor based on SBC. Results for the final selected model are shown in Table VI.

Removal of the latitude factor reduces the global covariate parameters to a small degree, while increasing $\gamma_{1c}$. The parameter variances also increase slightly. These results are expected, since we are moving the variance explained by the latitude factor into the unexplained variance, which shows as an increase in

Table V. Estimated changes to SBC and AIC during backward elimination. $\Delta\mathrm{AIC}_\mathrm{B} = W - 2q$ and $\Delta\mathrm{SBC}_\mathrm{B} = W - q \log(40 \times 94) = W - 8.23q$

| Model | Factor removed | Resulting model | Number of levels ($q$) | Information changes | |
|---|---|---|---|---|---|
| | | | | $\Delta\mathrm{AIC}_\mathrm{B}$ | $\Delta\mathrm{SBC}_\mathrm{B}$ |
| 4 | latitude | 2 | 5 | 10.9 | −20.3 |
| 4 | longitude | 3 | 8 | 95.2 | 45.3 |
| 2 | longitude | 1 | 8 | 92.5 | 42.6 |

Table VI. Parameter coefficients after final model selection

| | Value | Standard error | $t$ value | Units |
|---|---|---|---|---|
| $\gamma_{0h}$ | 0.359 | 0.015 | 24.78 | per hurricane |
| $\gamma_{0v}$ | 0.289 | 0.017 | 16.64 | per hurricane |
| $\gamma_{1c}$ | 0.084 | 0.020 | 4.09 | per hurricane |
| Intercept | 143.278 | 19.335 | 7.41 | |
| $\mathrm{long}_1$ | −0.111 | 0.077 | −1.44 | |
| $\mathrm{long}_2$ | −0.014 | 0.034 | −0.40 | |
| $\mathrm{long}_3$ | −0.008 | 0.020 | −0.41 | |
| $\mathrm{long}_4$ | −0.006 | 0.013 | −0.44 | |
| $\mathrm{long}_5$ | −0.015 | 0.010 | −1.54 | |
| $\mathrm{long}_6$ | −0.033 | 0.009 | −3.83 | |
| $\mathrm{long}_7$ | −0.038 | 0.008 | −4.64 | |
| $\mathrm{long}_8$ | −0.054 | 0.008 | −6.73 | |
| Warm | −0.222 | 0.041 | −5.37 | |
| Cold | 0.183 | 0.028 | 6.48 | |
| Dakar | 0.740 | 0.072 | 10.29 | years per metre |
| Azores | −0.115 | 0.014 | −8.40 | per millibar |
| Iceland | −0.027 | 0.008 | −3.66 | per millibar |

 

parameter variance. Note that although removing the latitude factor reduces the SBC, it increases the AIC; so, we keep the full model when using it to make forecasts.

## 7. MODEL FIT ISSUES AND HINDCASTS

### *7.1. Strong coupling*

Because of the strong couplings, we need to modify the parameter estimator. We find that some of the simulations at each time period contain large predicted values for hurricane activity. Thus, we remove simulations in the case that any cell contained the maximum value, $M = 10$, of the right truncated Poisson distribution. The restriction is reasonable, since the maximum observed number of hurricanes for any region during any year at any of the three regions' size is four. The restriction biases the estimator, in that the parameters are estimated for the spatial distribution conditioned on the maximum at any location being less than ten. This restriction will decrease the observed Fisher information, which will tend to inflate the values of the estimated standard error.

### *7.2. Grid size*

As mentioned above, the spatial grid is a compromise between sample size and resolution. We experimented with smaller grid boxes, but found that the MCMLE did not converge. In this case we lack accurate information for estimating the coupling parameters. The $6^\circ \times 6^\circ$ model converges, and we do not need to remove any observations, but the estimator rejects some of the samples at each stage. Using a larger neighbourhood might allow us to use smaller grid boxes.

We experimented with larger spatial neighbourhoods by adding the current period's four diagonal neighbour sites using a single parameter to the model. These sites are the NE, SE, SW and NW neighbour regions, with parameter $\gamma_{0\mathrm{d}}$ (the diagonal term). We have the same model described by Equation (2), with Equation (3) changed to

$$\begin{aligned}\log(\lambda_{t,ij}) = {} & \mathrm{C}_{ij}(t) + \gamma_{0\mathrm{h}}(H_{t,i+1,j} + H_{t,i-1,j}) + \gamma_{0\mathrm{v}}(H_{t,i,j+1} + H_{t,i,j-1}) \\ & + \gamma_{0\mathrm{d}}(H_{t,i+1,j+1} + H_{t,i-1,j+1} + H_{t,i-1,j-1} + H_{t,i+1,j-1}) + \gamma_{1\mathrm{c}}(H_{t-1,i,j})\end{aligned}$$

and the local neighbourhood of site $(t, ij)$, $h_{\partial(t,ij)}$, is the vector of nine response values.

We run the modified MCMLE for several iterations, using the previous values of the parameter estimates from the full model in Table III, and an initial MPLE estimate for $\gamma_{0\mathrm{d}}$ of 0.0 We estimate that $\gamma_{0\mathrm{d}} = 0.090$, $\sigma_{\gamma_{0\mathrm{d}}} = 0.021$, $t = 4.3$. Adding the diagonal parameter to the model significantly affects only the estimates for $\gamma_{0\mathrm{h}}$ and $\gamma_{0\mathrm{v}}$, reducing them to 0.319 and 0.209 respectively, while increasing their standard errors to 0.017 and 0.026 respectively. The correlation matrix of the coupling parameters and the intercept shows that, though the other terms have correlations less than 0.07 with each other, $\gamma_{0\mathrm{d}}$ is significantly correlated. This term is not only significant, but improves the model. If this term is added, both the estimated AIC and SBC are reduced by 17.2 and 10.9 respectively. Thus, future models should consider both larger spatial and temporal neighbourhoods.

There are concerns about increasing the size of the neighbourhood. If the new couplings are positive the estimator may fail to converge. Because we have more site values, the model will required additional boundary values and parameters. One may reduce the number of parameters by using combinations of various canonical parameters. For example, the parameter $\gamma_{0\mathrm{d}}$ is really the sum of two parameters: one for the NW–SE diagonal and another for the NE–SW diagonal.

### *7.3. Hindcasts*

The model can be used to forecast hurricane activity when lagged values of the covariates are included. At each stage of the MCMLE, we generate samples from the distribution of $\mathbf{X}_t$ conditioned on $\{\mathbf{X}_s : s < t\}$

 

using the observations $\{\mathbf{X}_{t-1}, \ldots, \mathbf{X}_{t-p}\}$, the covariates at time $t$, $z_k(t)$, $k = 1, \ldots, P$ the model parameters and estimated boundary values. For our application we use the full model parameters given in Table III, so as to have the smallest prediction error. Also, we estimate the boundary values using the mean for each cell.

As a single test case, we generate 103 sample forecasts of hurricane activity for 1994 in each $6^\circ \times 6^\circ$ region of grid $S$ using the 1994 values of the five global covariates. Hurricane activity during 1994, which was below the long-term average, is not included at any phase of model development. The spatial distribution and intensity of hindcast values are plotted in Figure 6. Table VII shows the mean and standard deviation for each region, along with a comparison with the observed 1994 values for that region. In Table VII, if at least one 1994 hurricane entered the grid box the observed value is set to one. Results indicate reasonable agreement with observations. In general, the hindcast indicates a greater mean value in grid boxes that were actually hit. Similarly, hindcasts were made on the 1995, 1996, and 1997 hurricane seasons.

A quantitative measure of hindcast skill for each year is the Brier skill score (SS), given as

$$\mathrm{SS} = 1 - \frac{\frac{1}{n}\sum_{k=1}^{n}(y_k - o_k)^2}{\frac{1}{n}\sum_{k=1}^{n}(c_k - o_k)^2} \tag{4}$$

where $y_k$ is the model probability, $o_k$ is the observed value, and $c_k$ is the climatological probability (see Wilks, 1995). Here the observed value is set to one if at least one hurricane entered the grid box and zero otherwise. The model and climatological probabilities are determined from their respective rates using the Poisson distribution. The value of SS is expressed as a percentage improvement over climatology for the forecast model. The Brier SS are 13.1%, 24.8%, 13.8%, and −0.7% for the years 1994, 1995, 1996, and 1997

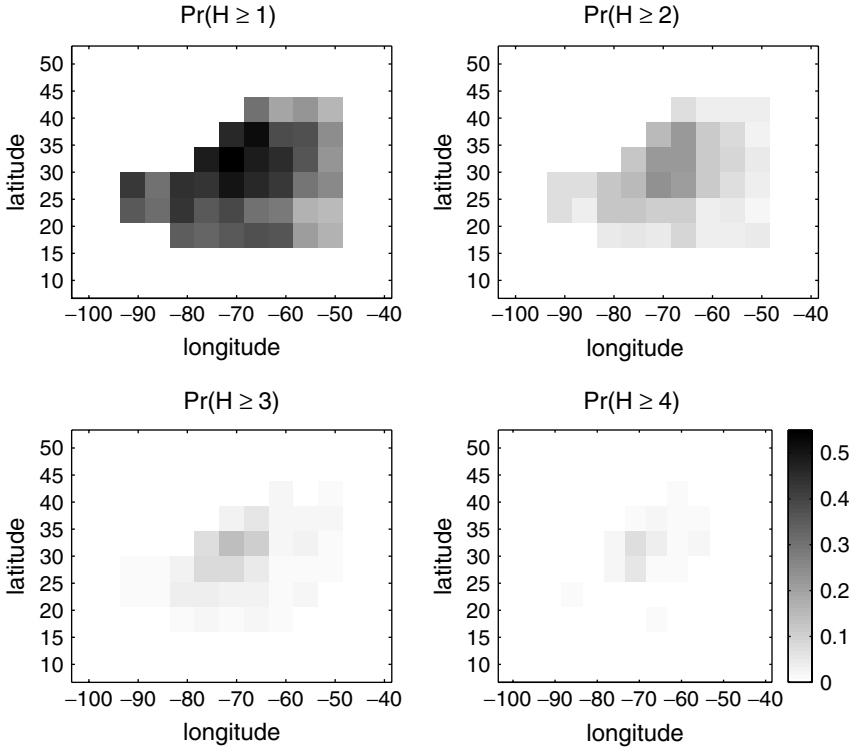


Figure 6. Probabilistic hindcasts of hurricane activity for the 1994 North Atlantic hurricane season. Grey levels indicate the hindcast probability that a given region will have $H$ or more hurricanes

 

Table VII. Hindcasts of the 1994 North Atlantic hurricane season by region

| Region centre | Sample | | Actual value | Region centre | Sample | | Actual value |
|---|---|---|---|---|---|---|---|
| | Mean | SD | | | Mean | SD | |
| 83 °W 15 °N | 0.398 | 0.616 | 0 | 71 °W 27 °N | 0.864 | 1.121 | 0 |
| 77 °W 15 °N | 0.408 | 0.663 | 1 | 65 °W 27 °N | 0.728 | 0.972 | 0 |
| 71 °W 15 °N | 0.408 | 0.617 | 0 | 59 °W 27 °N | 0.553 | 0.763 | 0 |
| 65 °W 15 °N | 0.495 | 0.803 | 0 | 53 °W 27 °N | 0.369 | 0.642 | 0 |
| 59 °W 15 °N | 0.408 | 0.601 | 0 | 47 °W 27 °N | 0.301 | 0.575 | 0 |
| 53 °W 15 °N | 0.243 | 0.514 | 0 | 77 °W 33 °N | 0.699 | 0.968 | 0 |
| 47 °W 15 °N | 0.214 | 0.517 | 0 | 71 °W 33 °N | 1.000 | 1.358 | 1 |
| 95 °W 21 °N | 0.427 | 0.651 | 0 | 65 °W 33 °N | 0.854 | 1.175 | 1 |
| 89 °W 21 °N | 0.369 | 0.642 | 0 | 59 °W 33 °N | 0.592 | 0.785 | 0 |
| 83 °W 21 °N | 0.592 | 0.810 | 0 | 53 °W 33 °N | 0.505 | 0.862 | 0 |
| 77 °W 21 °N | 0.515 | 0.815 | 1 | 47 °W 33 °N | 0.282 | 0.584 | 0 |
| 71 °W 21 °N | 0.524 | 0.765 | 0 | 71 °W 39 °N | 0.641 | 0.838 | 0 |
| 65 °W 21 °N | 0.437 | 0.763 | 0 | 65 °W 39 °N | 0.835 | 1.103 | 0 |
| 59 °W 21 °N | 0.330 | 0.584 | 0 | 59 °W 39 °N | 0.563 | 1.026 | 1 |
| 53 °W 21 °N | 0.233 | 0.597 | 0 | 53 °W 39 °N | 0.476 | 0.739 | 0 |
| 47 °W 21 °N | 0.165 | 0.422 | 0 | 47 °W 39 °N | 0.291 | 0.588 | 0 |
| 95 °W 27 °N | 0.495 | 0.655 | 0 | 65 °W 45 °N | 0.369 | 0.610 | 0 |
| 89 °W 27 °N | 0.379 | 0.643 | 0 | 59 °W 45 °N | 0.262 | 0.641 | 0 |
| 83 °W 27 °N | 0.592 | 0.785 | 1 | 53 °W 45 °N | 0.262 | 0.523 | 0 |
| 77 °W 27 °N | 0.670 | 0.974 | 1 | 47 °W 45 °N | 0.204 | 0.531 | 0 |

respectively. The 1995 and 1996 hurricane seasons were quite active (11 and 9 hurricanes respectively) and show the largest SS. The 1994 and 1997 season were inactive, each having only three hurricanes. Only the 1997 season indicates no improvement over climatology. Overall, the hindcast results support the contention that the TPSTAR model, or similar spatial count models, might be useful in predicting regional hurricane activity over the North Atlantic basin.

## 8. SUMMARY AND CONCLUSIONS

We introduce and apply a space–time count process model to North Atlantic hurricane activity. The model uses the best-track data consisting of historical hurricane positions and intensities together with climate variables to determine local space–time coefficients of a truncated Poisson process. The model, referred to as a TPSTAR model, is motivated by first examining a time-series model for the entire domain. Then a Poisson GLM is considered that uses grid boxes within the domain and adds offset factors for latitude and longitude. A natural extension is then made that includes instantaneous local and autoregressive coupling between the grids. A final version of the model is found by backward selection of the predictors based on values of SBC and AIC. Hindcasts are performed on the 1994–97 hurricane seasons using a model having five nearest neighbours and statistically significant couplings. The parameters in the TPSTAR model are estimated using MPLE. Brier SS indicates model skill above climatology during three of the four years. The model shows promise as a potential forecast tool.

Several conclusions concerning the application of the TPSTAR model to seasonal North Atlantic hurricane activity are reached:

- Seasonal hurricane activity over the North Atlantic basin can be modelled as a space–time Poisson process.
- There appears to be some hurricane path persistence between seasons.
- Dividing the region into grid boxes and adding coupling increases the significance of the global predictors.

 

- Increasing the neighbourhood size can improve the model at the cost of estimating additional parameters and boundary values.
- From the MCML estimates, $t$ tests can be performed to determine if the instantaneous couplings are significant. If they are not we can use the simpler Poisson GLM model.
- Grid size is important to the model formulation. The spatial parameters $\gamma_{0v}$ and $\gamma_{0h}$ do not scale with changing grid size, and the MCMLE may fail to converge for small grid size.
- A hindcast case study indicates some skill above climatology, providing evidence that the TPSTAR modelling procedure can be useful as a climate prediction tool.

## ACKNOWLEDGMENTS

The study was partially funded by the National Science Foundation (ATM-0086958) and the Risk Prediction Initiative of the Bermuda Biological Station for Research (RPI-99-001).

## REFERENCES

Arguez A, Elsner JB. 2001. Trends in U.S. tropical cyclone mortality during the 20th century. *The Florida Geographer* in press.
Bartlett MS. 1968. A further note on nearest-neighbor models. *Journal of the Royal Statistical Society A* **131**: 579–580.
Besag JE. 1974. Spatial interaction and the statistical analysis of lattice systems. *Journal of the Royal Statistical Society B* **36**: 192–225.
Brockwell P, Davis A. 1991. *Time Series: Theory and Methods*, 2nd edn. Springer-Verlag: New York.
Elsner JB, Bossak BH. 2001. Bayesian analysis of U.S. hurricane climate. *Journal of Climate* **14**: 4341–4350.
Elsner JB, Bossak BH. 2002. Changes in hurricane landfall probabilities in response to variations in climate. In *Hurricanes and Typhoons: Past, Present, and Future*, Murnane RJ, Liu Kb (eds). Columbia University Press: in press.
Elsner JB, Kara AB. 1999. *Hurricanes of the North Atlantic: Climate and Society*. Oxford University Press: New York.
Elsner JB, Lehmiller GS, Kimberlain TB. 1996. Early August forecasts of Atlantic tropical storm activity for the balance of the 1996 season, using Poisson models. *Experimental Long-lead Forecast Bulletin* **5**(3): 26–28.
Elsner JB, Niu XF, Tsonis AA. 1998. Multi-year prediction model of North Atlantic hurricane activity. *Meteorology and Atmospheric Physics* **68**: 42–51.
Elsner JB, Liu Kb, Kocher B. 2000. Spatial variations in major U.S. hurricane activity: statistics and a physical mechanism. *Journal of Climate* **13**: 2293–2305.
Elsner JB, Bossak BH, Niu XF. 2001. Secular changes to the ENSO–U.S. hurricane relationship. *Geophysical Research Letters* **28**: 4123–4126.
Geyer CM. 1994. On the convergence of Monte Carlo maximum likelihood calculations. *Journal of the Royal Statistical Society B* **56**: 261–274.
Gilks WR, Richardson S, Spiegelhalter DJ. 1996. *Markov Chain Monte Carlo in Practice*. Chapman & Hall: London.
Gray WM. 1984. Atlantic seasonal hurricane frequency: part II. Forecasting its variability. *Monthly Weather Review* **112**: 1669–1683.
Jagger TH. 2000. *A truncated space–time autoregressive model. Ph.D. Thesis*, Department of Statistics, Florida State University.
Jagger TH, Elsner JB, Niu XF. 2001. A dynamic probability model of hurricane winds in coastal counties of the United States. *Journal of Applied Meteorology* **40**: 853–863.
Landsea CW, Gray WM. 1992. The strong association between Western Sahel monsoon rainfall and intense Atlantic hurricanes. *Journal of Climate* **5**: 435–453.
Lehmiller GS, Kimberlain TB, Elsner JB. 1997. Seasonal prediction models for North Atlantic basin hurricane location. *Monthly Weather Review* **125**: 1780–1791.
Neumann CJ, Jarvinen BR, McAdie CJ, Hammer GR. 1999. *Tropical cyclones of the North Atlantic Ocean, 1871–1998*. National Oceanic and Atmospheric Administration.
Sharpiro LJ. 1987. Month-to-month variability of the Atlantic tropical circulation and its relationship to tropical storm formation. *Monthly Weather Review* **115**: 2598–2614.
Whittle P. 1963. Stochastic processes in several dimensions. *Bulletin of the International Statistical Institute* **40**: book 2.
Wilks DS. 1995. *Statistical Methods in the Atmospheric Sciences*. Academic Press: San Diego.
Winkler G. 1995. *Image Analysis, Random Fields, and Dynamic Monte Carlo Methods*. Springer-Verlag: Berlin.
Wu H. 1994. *Regression models for spatial binary data with application to the distribution of plant species. Ph.D. Thesis*, Department of Statistics, Florida State University.

 